[5] J. P. Costes, F. Dahan, B. Donnadieu, J. Garcia-Tojal, J. P. Laurent, *Eur. J. Inorg. Chem.* **2001**, 363.

[6] A. Panagiotopoulos, T. F. Zafiropoulos, S. P. Perlepes, E. Bakalbassis, I. Masson-Ramade, O. Kahn, A. Terzis, C. P. Raptopoulou, *Inorg. Chem.* **1995**, *34*, 4918, and references therein.

[7] R. Hedinger, M. Ghisletta, K. Hegetschweiler, E. Toth, A. E. Merbach, R. Sessoli, D. Gatteschi, V. Gramlich, *Inorg. Chem.* **1998**, *37*, 6698.

[8] J. P. Costes, F. Dahan, F. Nicodème, *Inorg. Chem.* **2001**, *40*, 5285.

[9] S. Liu, L. Gelmini, S. J. Rettig, R. C. Thompson, C. Orvig, *J. Am. Chem. Soc.* **1992**, *114*, 6081.

[10] P. Guerriero, S. Tamburini, P. A. Vigato, C. Benelli, *Inorg. Chim. Acta* **1991**, *189*, 19.

[11] J. P. Costes, A. Dupuis, J. P. Laurent, *Inorg. Chim. Acta* **1998**, *268*, 125.

[12] To our knowledge, the two sets of data have been reported for a binuclear species,[9] for $[Gd_2(thd)_6]$ (thd = 2,2,6,6-tetramethylheptanedionato)[11] (see ref. [13] for the structural determination) and for two trinuclear complexes.[7,8] In all compounds, the ground state is antiferromagnetic with J values between -0.045 and -0.21 cm^{-1}.

[13] I. Baxter, S. R. Drake, H. B. Hursthouse, K. M. Abdul Malik, J. McAleese, D. J. Otway, J. Plakatouras, *Inorg. Chem.* **1995**, *34*, 1384.

[14] Crystal structure analysis: The data were collected on an Enraf-Nonius CAD4 diffractometer with $Mo_{K\alpha}$ radiation. The structure was solved using Patterson techniques (SHELXS97) and refined on F^2 (SHELXL-97). **1**: $C_{42}H_{46}Er_2O_{26}$, $M_r = 1301.31$, triclinic, space group $P\bar{1}$, $a = 9.9231(11)$, $b = 14.313(2)$, $c = 9.4312(13)$ Å, $\alpha = 91.663(16)$, $\beta = 115.677(14)$, $\gamma = 99.054(13)^\circ$, $V = 1185.0(3)$ Å^3, $Z = 1$, $\rho_{calcd} = 1.823$ Mg m^{-3}, $F(000) = 642$, $\lambda = 0.71073$ Å, $\mu(Mo_{K\alpha}) = 3.608$ mm^{-1}, $T = 293$ K, crystal size $0.45 \times 0.35 \times 0.20$ Å^3. 5153 collected reflections are unique; max./min. residual electron density $0.837/-0.682$ e Å^3, $R1 = 0.0158$ ($F_o^2 > 2\sigma(F_o^2)$), wR2 = 0.0434 (all data). Crystallographic data (excluding structure factors) for the structure reported in this paper have been deposited with the Cambridge Crystallographic Data Centre as supplementary publication no. CCDC-163647. Copies of the data can be obtained free of charge on application to CCDC, 12 Union Road, Cambridge CB2 1EZ, UK (fax: (+44) 1223-336-033; e-mail: deposit@ccdc.cam.ac.uk).

[15] J. H. Burns, W. H. Baldwin, *Inorg. Chem.* **1977**, *16*, 289.

[16] M. Jian-Fang, J. Zhong-Sheng, N. Jia-Zuan, *Chin. J. Struct. Chem.* **1991**, *10*, 125.

[17] M. A. Nabar, S. D. Barve, *J. Crystallogr. Spectrosc. Res.* **1984**, *14*, 341.

[18] See, for example: A. Ouchi, Y. Suzuki, Y. Ohki, Y. Koizumi, *Coord. Chem. Rev.* **1988**, *92*, 29.

[19] P. Pascal, *Ann. Chim. Phys.* **1910**, *19*, 5.

[20] The LASIP diffractometer has a geometry specially set up for scattering measurements. It minimizes every external parasite scattering phenomenon. Experimental details are given in the Supplementary Material.

Foldamers as Dynamic Receptors: Probing the Mechanism of Molecular Association between Helical Oligomers and Rodlike Ligands**

Aya Tanatani, Thomas S. Hughes, and Jeffrey S. Moore*

The helix is one of the most significant structural motifs observed in biological[1] and synthetic[2] polymers. We have previously shown that *m*-phenylene ethynylene oligomers **1** exhibit unique helical structures in polar solvents[3] and possess a cavity which can bind hydrophobic molecules.[4] The rodlike ligand **2** exhibited affinities to **1** that were dependent on either the length of the oligomer or the height

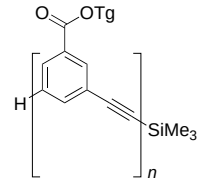

1 (*n* = 16, 18, 20, 22, 24)

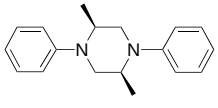

2

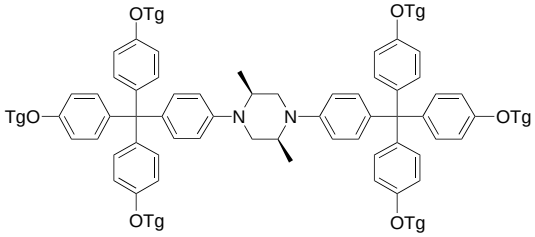

3: Tg = $(CH_2CH_2O)_3CH_3$

of the helical cavity. The association constants rose steadily as the length of the oligomer increased from the decamer to the octadecamer but then reached a plateau, with a weak maximum at the icosamer. Only nonspecific, nondirectional solvophobic interactions stabilize these complexes.

Intuitively, a capped rod, namely, a dumbbell-shaped ligand, may exhibit greater specificity by blocking the strong binding of oligomers which are too long to fit between the caps. However, the ability of capped rods to function as ligands depends on the presence of a kinetically accessible complexation pathway. Two possible limiting mechanisms can be imagined in a polar solvent that favors the folded state of **1**:

[*] Prof. J. S. Moore, Dr. A. Tanatani, Dr. T. S. Hughes
Roger Adams Laboratory
Departments of Chemistry and Materials Science & Engineering
University of Illinois at Urbana-Champaign
600 South Mathews Avenue, Urbana, Illinois 61801 (USA)
Fax: (+1) 217-244-8068
E-mail: moore@scs.uiuc.edu

[**] This research was funded by the National Science Foundation (Grant CHE 00-91931). A.T. acknowledges the support of the Japan Society for the Promotion of Science in the form of a Fellowship for Japanese Junior Scientists. The authors gratefully acknowledge Dr. Petr Kuzmic for customizing his program *Dynafit* to facilitate our data analysis.

Supporting information for this article is available on the WWW under http://www.angewandte.com or from the author.

  1433-7851/02/4102-0325 $ 17.50+.50/0

1) the chiral ligand threads into the helical cavity of a rigid oligomer, or 2) a transiently unfolded oligomer winds around the chiral ligand (Figure 1 a). This mechanistic question parallels that asked of many biological systems; that is, how much reorganization of the folded receptor occurs upon binding?[5] Here, we describe the high affinity and high specificity of a dumbbell-shaped ligand, whose shape should mimic the mode of binding of **2** to **1** and restrict the possible mechanisms of complexation.

The dumbbell-shaped ligand **3** consists of *N*,*N*′-diphenylpiperazine **2** capped with triarylmethyl moieties at both ends of the rod. Each terminal aryl group was *para* substituted with triglyme (Tg) ethers to improve solubility. The ends of this molecule should be too bulky to enter the cavity of a rigid helical oligomer by threading (Figure 1 b).[6] This assumption was evaluated by molecular modeling; structures of the ligand and helical oligomer were optimized by molecular mechanics.[7] The diameter of the helical cavity was calculated to be 8.7 Å, while the diameter of the capping group (without side chains) was calculated to be 10.2 Å. By comparison, the diameter of the piperazine portion of the ligand was about 6.6 Å. Therefore, the observation of a high binding affinity between **3** and oligomer **1** would suggest that a dynamic mechanism such as pathway (2) (Figure 1 a) is viable.

The synthesis of dumbbell-shaped molecule **3** is illustrated in Scheme 1. Triarylmethanol **4** was prepared in 72% yield by the reaction of methyl 4-bromobenzoate with *p*-methoxyphenylmagnesium bromide. Bis(tetraarylmethane) **5a** was obtained in 50% yield by treatment of **4** in phenol with a catalytic amount of HBr according to the procedure reported by Gibson et al.[8] It should be noted that the use of a catalytic amount of HCl resulted in a 1:1 mixture of **5a** and **5b**. After removal of the methyl groups by treatment with BBr_3 in CH_2Cl_2 (93% yield), etherification of **6** with triglyme under Mitsunobu conditions[9] gave **7** in 47% yield. Buchwald–Hartwig amination of **7** with (2*S*,5*S*)-2,5-dimethylpiperazine afforded the monoadduct **8** (45% yield) and target **3**, albeit in low yield (10%). No epimerization of the piperazine ring was observed during amination.

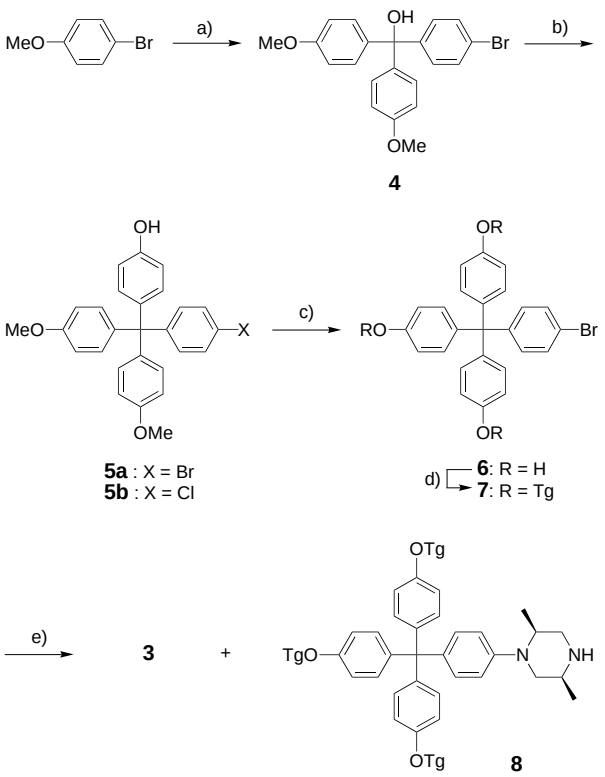

Scheme 1. Synthesis of dumbbell-shaped ligand **3**: a) Mg, diethyl ether, 40 °C, 12 h; methyl 4-bromobenzoate, 40 °C, 18 h, 72%; b) phenol, HBr, 120 °C, 16 h, 50%; c) BBr_3, CH_2Cl_2, RT, 2 h, 93%; d) $CH_3(OCH_2CH_2)_3OH$, diethylazodicarboxylate, Ph_3P, THF, RT, 18 h, 47%; e) $[Pd_2(dba)_3]$, NaO*t*Bu, 2-diphenylphosphanyl-2′-dimethylaminobiphenyl, *cis*-(2*S*,5*S*)-2,5-dimethylpiperazine, toluene, 85 °C, 18 h, 10% of **3**. dba = dibenzylideneacetone.

Induced circular dichroism (CD) signals were observed upon mixing solutions of **3** and the members of oligomer series **1** ($n = 16$, 18, 20, 22, 24), which indicates that the presence of the capping groups did not prevent association. Figure 2 (inset) shows a representative series of spectra obtained from the addition of different concentrations of

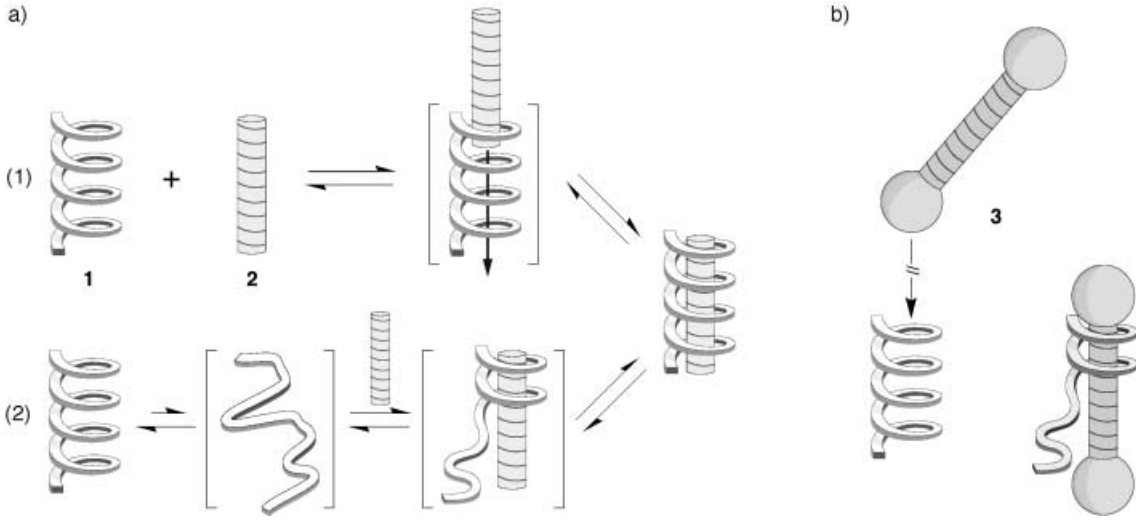

Figure 1. Foldamer association with rodlike ligands. a) Two possible limiting mechanisms are the static, rigid case in which the chiral ligand threads through the cavity of the helical oligomer without disruption of the helical structure (1), and the dynamic, flexible case in which the unfolded or partially folded oligomer winds around the chiral ligand (2). b) Mechanistic probe.

  1433-7851/02/4102-0326 $ 17.50+.50/0 *Angew. Chem. Int. Ed.* **2002**, *41*, No. 2

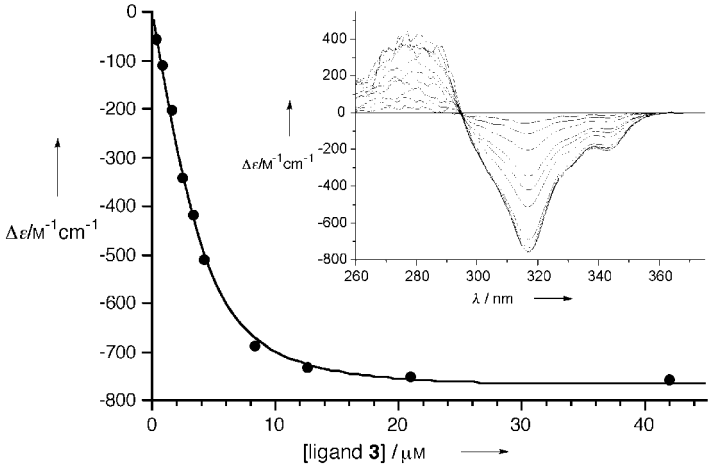

Figure 2. Plot of the $\Delta\varepsilon$ value at 317 nm against the concentration of ligand **3** for its association with oligomer **1** ($n = 20$) in 40% H_2O in CH_3CN at 294 ± 1 K. [**1**] = 4.2 μM. The points represent the observed data, while the line represents the nonlinear least-squares fit. The inset shows the corresponding CD spectra.

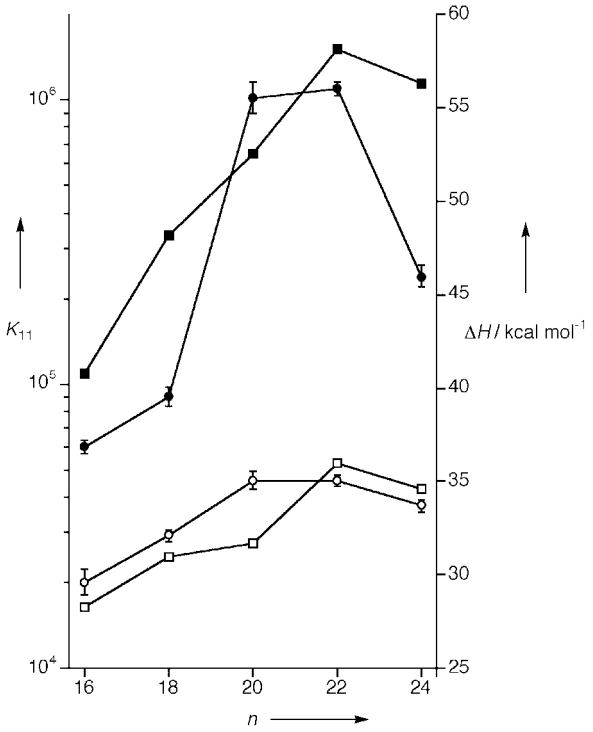

Figure 3. Plot of $\log K_{11}$ values (circles) and modeled heat of association (squares) against oligomer length for ligands **2** and **3**. Experimental K_{11} values for **2** (○) are taken from ref. [4b] for direct comparison to **3** (●). All measurements were recorded in a mixed solvent of 40% H_2O in CH_3CN at 294 ± 1 K. [**1**] = 4.2 μM. □ represents the calculated heat of association for **2** and ■ for **3**. The energy scale is arbitrary since no contribution from the entropy of binding is included.

enantiomerically pure **3** to the icosamer in 40% aqueous acetonitrile. The CD spectra were very similar to those observed for the 1:1 complex formed between **2** and **1**,[4b] and the stoichiometry of the complex formed between **3** and **1** was also determined to be 1:1 from the quality of the nonlinear least-squares fitting to the 1:1 binding isotherm.[10][11]

The binding affinities of **3** for members of oligomer series **1** were determined by these nonlinear fits.[12] As shown in Figure 3, the value of the association constant K_{11} increased as the length of the oligomer increased from the hexadecamer to the docosamer.[13] The length dependence of the association constants and the similarity of the CD spectra to those observed previously for the 1:1 complex formed between **2** and **1** suggest that dumbbell-shaped ligand **3** also binds within the helical cavity of the folded oligomer rather than in some alternative geometry, such as transversely through the turns of the helix or to a nonhelical conformation. The K_{11} value of **3** with the icosamer of **1**[14] was calculated to be $(1.0 \pm 0.1) \times 10^6\ \text{M}^{-1}$. This value is more than 20 times stronger than the K_{11} value of **2** with the icosamer. Not only is the affinity of **1** for ligand **3** larger than that of ligand **2** at each oligomer length, the specificity of ligand **3** towards oligomers of different lengths is also much greater than that of ligand **2**.[15] For example, in the case of rodlike ligand **2**, the association of the icosamer is only 2.3 times larger than that of the hexadecamer. However, this ratio is about 20:1 for dumbbell-shaped ligand **3**. This specificity can easily be seen in Figure 3; the maximum in the plot of the K_{11} value versus oligomer length is much more pronounced for **3** than for **2**.

We previously assumed that the affinity depends on the area of contact between the interacting molecular surfaces, given the absence of any obvious, specific, directional interactions.[4b] The predicted enthalpy of binding from molecular mechanics models[16] increased nearly linearly as the oligomer increased in size from the hexadecamer to the docosamer, but decreased for the tetracosamer. Just as for the **1**·**2** complexes, no specific intermolecular interactions were evident in the modeled **1**·**3** complexes, with the exception of possible aromatic–aromatic interactions between the terminal oligomeric phenyl rings and the phenyl rings of the trityl capping group. The modeled structures of all of the complexes **1**(n = 16–20)·**3** revealed the ligand could be encapsulated within a completely helical oligomer, whereas the **1**($n = 24$)·**3** complex could only form upon some twisting of the terminal oligomeric phenyl groups out of the ideal helical conformation. The fully folded hexadecamer and octadecamer are too short to interact with both of the capping groups; the affinity is thus relatively low and the specificity for these lengths not very high. However, the icosamer and docosamer are long enough to potentially form energetically favorable contacts with both tetraarylmethane capping groups. These stabilizing interactions may be responsible for the large differences between the K_{11} values of ligands **2** and **3**, and the high chain length specificity. The lower binding constant for the tetracosamer, as well as the perturbation of the helical structure of the oligomer in the model of the **1**($n = 24$)·**3** complex suggests that the helix may be too long to fit between the capping groups in its fully folded state. It is possible that some deformation occurs to accommodate **3**, such as alteration of the pitch of the helix or fraying of the helix ends as seen in the model.

The kinetics of the association of **1** with **2** and with **3** were examined to further probe the mechanism of complexation. As can be seen in Figure 4, the diastereomeric excess of the **1**($n = 20$)·**2** complex is already present by the time the first measurement is made at 60 seconds after mixing, and does not

  1433-7851/02/4102-0327 $ 17.50+.50/0

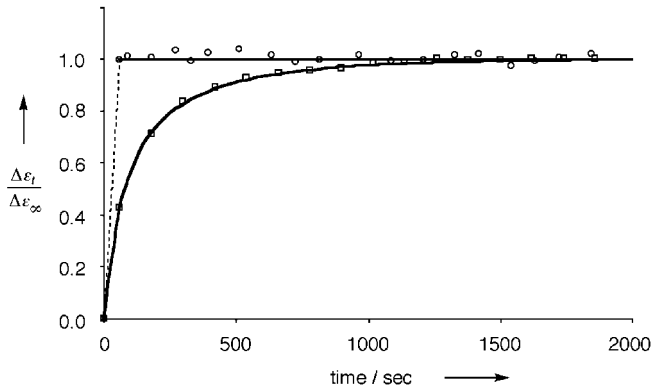

Figure 4. Kinetics of complexation of **2** and **3** with **1**. The percentage of the equilibrium signal is shown as a function of the time after mixing the ligand and the oligomer. □ represents the formation of the complex of **3** with **1** while ○ represents the complex of **2** with **1**. The solid lines are nonlinear fits to the data using a second-order kinetic model. The dashed line indicates the absence of data for very short reaction times; the shape of the kinetic curve in this region is undetermined. [**1**] = 4 μM, [**2**] = 45 μM, [**3**] = 10 μM in 40% H_2O in CH_3CN.

change appreciably over the next thirty minutes. This observation suggests that the binding event is rapid, as is possible for a direct threading mechanism such as pathway (1) in Figure 1. Different kinetic behavior is observed for the association of **1** and **3**.

The growth of the CD signal was slower for the association of **1** with **3** (Figure 4). It is reasonable to assume that the slower establishment of the diastereomeric equilibrium is the result of the greater degree of oligomer chain reorganization required to accommodate ligand **3** within the helical cavity. The transition state for this association would be both entropically disfavored, because of the chain movements required, and enthalpically disfavored, because of the disruption of the enthalpically favored helical state. The fact that association does occur for **3** indicates that a mechanism which involves a dynamic receptor, such as pathway (2) in Figure 1 a, is a viable process for foldamers **1**. The different kinetic behavior exhibited by the two ligands suggests that **1** and **2** associate by a mechanism more like pathway (1) in Figure 1 a, but a pathway that involves significant chain reorganization (pathway (2)) cannot be ruled out.

In conclusion, we have demonstrated that the addition of capping groups to rodlike ligand **2** to yield the dumbbell-shaped ligand **3** does not block its binding to foldamers **1** and has large, length-specific association energies. This result allows the mechanistic conclusions that a dynamic pathway is accessible for the inclusion of hydrophobic molecules in the helical cavity of **1**, and that the molecular recognition by helical foldamers involves at least some deformation of the fully folded helix. It remains to be shown if reorganization of the helix is required or indeed kinetically competitive for systems in which pathway (1) is allowed. Furthermore, the higher affinity and oligomer length specificity of **3** relative to **2** may allow its use as a template for size-selective dynamic syntheses[17] of foldamers structurally similar to **1**.

Received: June 26, 2001
Revised: October 5, 2001 [Z17359]

[1] G. Quinkert, E. Egert, C. Griesinger, *Aspects of Organic Chemistry*, VCH, Basel **1996**.
[2] W. L. Mattice, V. W. Suter, *Conformational Theory of Large Molecules: The Rotational Isomeric State Model in Macromolecular Systems*, Wiley, New York **1994**; H.-M. Müller, D. Seebach, *Angew. Chem.* **1993**, *105*, 483; *Angew. Chem. Int. Ed. Engl.* **1993**, *32*, 477.
[3] a) J. C. Nelson, J. G. Saven, J. S. Moore, P. W. Wolynes, Science **1997**, *277*, 1793; b) R. B. Prince, J. G. Saven, J. S. Moore, P. W. Wolynes, *J. Am. Chem. Soc.* **1999**, *121*, 3114.
[4] a) R. B. Prince, S. A. Barnes, J. S. Moore, *J. Am. Chem. Soc.* **2000**, *122*, 2758; b) A. Tanatani, M. J. Mio, J. S. Moore, *J. Am. Chem. Soc.* **2001**, *123*, 1792.
[5] R. S. Spolar, M. T. Record, Jr., *Science* **1994**, *263*, 777; D. Szwajkajzer, J. Carey, *Biopolymers* **1997**, *44*, 181; A. M. Davis, S. J. Teague, *Angew. Chem.* **1999**, *111*, 778; *Angew. Chem. Int. Ed.* **1999**, *38*, 737.
[6] C. Heim, A. Affeld, M. Nieger, F. Vögtle, *Helv. Chim Acta* **1999**, *82*, 746, and references therein.
[7] The MM2 force field implemented in MacroModel 7.0 included the GB/SA water solvation treatment, and was also modified to include a twofold 0.6 kcal mol^{-1} rotational barrier about all the diphenylacetylenic single bonds.[3a]
[8] H. W. Gibson, S.-H. Lee, P. T. Engen, P. Lecavalier, J. Sze, Y. X. Shen, M. Bheda, *J. Org. Chem.* **1993**, *58*, 3748.
[9] S. Lahiri, J. L. Thompson, J. S. Moore, *J. Am. Chem. Soc.* **2000**, *122*, 11315.
[10] K. A. Connors, *Binding Constants: The Measurement of Molecular Complex Stability*, Wiley, New York, **1987**; K. A. Connors, *Chem. Rev.* **1997**, *97*, 1325; R. S. Murphy, T. C. Barros, J. Barnes, B. Mayer, G. Marconi, C. J. Bohne, *J. Phys. Chem. A* **1999**, *103*, 137.
[11] Benesi–Hildebrand and Scatchard plots were also consistent with 1:1 binding, although they were nonlinear for the strongly binding oligomers. These plots are not expected to be linear at low ligand concentrations; the linearity of these plots is dependent on the assumption that at equilibrium $[\mathbf{3}] \approx [\mathbf{1}\cdot\mathbf{3}]+[\mathbf{3}]$.
[12] The program Dynafit was used for nonlinear least-squares fitting: P. Kuzmic, *Anal. Biochem.* **1996**, *237*, 260.
[13] The K_{11} value is actually the sum of the individual association constants of **3** to the right- and left-handed helices of **1**.
[14] The K_{11} value of the icosamer and the docosamer with **3** were also measured using 0.42 μM solutions of the oligomer and found to be identical within experimental error.
[15] We also observed that the saturation molar CD intensity with **3**, $\Delta\varepsilon_\infty$, also reached a maximum when the length of the oligomer reached the icosamer. This value was twice that observed for rodlike ligand **2** with the icosamer.
[16] The enthalpies of binding were calculated by subtracting the modified MM2 (see ref. [7]) enthalpies of the free ligand and the free helical oligomer at infinite separation from the enthalpy of the complex.
[17] J. S. Moore, N. W. Zimmerman, *Org. Lett.* **2000**, *2*, 915; Y. L. Cho, H. Uh, S.-Y. Chang, H.-Y. Chang, M.-G. Choi, I. Shin, K.-S. Jeong, *J. Am. Chem. Soc.* **2001**, *123*, 1258; J.-M. Lehn, A. V. Eliseev, *Science* **2001**, *291*, 2331.

  1433-7851/02/4102-0328 $ 17.50+.50/0